Available online at www.sciencedirect.com
ScienceDirect
Ceramics International 37 (2011) 2423–2427
CERAMICS INTERNATIONAL
www.elsevier.com/locate/ceramint

Giant dielectric constant in $Nd_2NiO_{4+\delta}$ ceramics obtained by spark plasma sintering

X.Q. Liu *, C.L. Song, Y.J. Wu, X.M. Chen

Department of Materials Science and Engineering, Laboratory of Dielectric Materials, Zhejiang University, Hangzhou 310027, China

Received 13 October 2010; received in revised form 3 March 2011; accepted 24 March 2011
Available online 27 May 2011

Abstract

The crystal structure and dielectric properties of $Nd_2NiO_{4+\delta}$ ceramics prepared by spark plasma sintering (SPS) process were characterized. The crystal structure belonged to orthorhombic system with a space group of *F mmm*, and the excess oxygen content, δ, was about 0.192. Temperature-stable giant dielectric constants ($\varepsilon' \sim 10^5$) up to high frequency (5 MHz) over a wide temperature range (200–500 K) were observed in the present ceramics. After comparing the activation energies of dielectric relaxation and electrical conduction, we found the giant dielectric response should be mainly attributed to the adiabatic small polaronic hopping process, while the polaronic hopping process was closely related to the charge ordering in the present ceramics.

Keywords: B. X-ray method; C. Dielectric properties; Spark plasma sintering; Charge ordering

1. Introduction

Charge/spin ordering is one of the most interesting phenomena in materials with strongly correlated electronic, and some fascinating physical properties, such as, colossal magnetoresistance and multiferroicity, are closely related to these orderings [1,2]. Among these materials, the compounds $Ln_{2-x}Sr_xNiO_{4+\delta}$ (Ln =La and Nd) have been intensively investigated because their structures are closely related to the superconducting compounds $La_{2-x}Sr_xCuO_4$ (Refs. [3–6]). In these compounds, the charge/spin orderings are observed over a wide hole concentration region, $0.15 \leq n_h = x + 2\delta \leq 0.5$, where, n_h is the hole concentration, x is the strontium content, and δ is the excess oxygen concentration. This indicates the excess oxygen plays the same role as that of substituted strontium ion. Upon cooling down to the charge ordering temperature, the holes will condense to form charge stripes. With further cooling down to the spin ordering temperature, the ordered spins appear. The ordered spins lay between the charge stripes, i.e., the charge stripes act as walls of the local ordered spin domains. The stripe order is most stable at $n_h = 1/3$, where the compound shows the highest charge and spin ordering temperature [7].

On the other hand, the giant dielectric constants ($\varepsilon' \sim 10^5$) up to high frequency have been discovered in $Ln_{3/2}Sr_{1/2}NiO_4$ (Ln = La, Nd, and Sm) ceramics. The giant dielectric constant should be mainly attributed to the adiabatic small polaronic hopping process, and the polaronic hopping process is closely related to the charge ordering in these materials [8,9]. Recently, the giant dielectric response up to high frequency is also observed in the $La_{2-x}Sr_xNiO_4$ ($x = 1/8$, $1/3$) single crystal, and results also show the dielectric response is closely related to the charge stripe ordering [10–12]. The giant dielectric response up to high frequency response is the unique characteristic of the nickelates with K_2NiF_4 structure, and this may allow a potential application of these materials at high frequencies. As shown in the previous work [3–6], the excess oxygen also can induce the charge ordering in nickelates, so the giant dielectric response should be observed in the compound with excess oxygen if the correlation between the giant dielectric response and charge ordering is definite. So in the present work, we prepare an oxygen-excess compound $Nd_2NiO_{4+\delta}$ by spark plasma sintering (SPS), and the correlation between the dielectric response and charge ordering is confirmed.

* Corresponding author. Tel.: +86 571 87951410; fax: +86 571 87951410.
E-mail address: xqliu@zju.edu.cn (X.Q. Liu).

0272-8842/$36.00
doi:10.1016/j.ceramint.2011.05.093

2. Experimental procedure

$Nd_2NiO_{4+\delta}$ powders were prepared by a solid-state reaction with using Nd_2O_3 (99.9%), and NiO (99%) as starting materials. The weighted raw materials were mixed by ball milling with ZrO_2 media in ethanol for 24 h, and then the dried mixtures were calcined at 1200 °C for 3 h to yield desired materials. The obtained powders were added into a graphite die and sintered at 950 °C for 5 min under a vacuum of 6 Pa with a SPS apparatus (SPS-1050, SPS Syntex Inc., Kanagawa, Japan). During the period of heating and soaking, a pressure of 30 MPa was applied on the sample. The heating rate was 100 °C/min from room temperature to 900 °C and 25 °C/min from 900 °C to 950 °C. Then the as-sintered samples were annealed in air at 600 °C for 2 h to remove the residual carbon on the surface of samples, and relatively dense ceramics were obtained. The crystalline phase was identified by powder X-ray diffraction (XRD) using Cu $K\alpha$ radiation (Rigaku D/max 2550 PC, Rigaku Co., Tokyo, Japan). The XRD data for Rietveld refinement were collected over a 2θ range of 8–130° with a step size of 0.02° and a count of time of 1 s. The Rietveld refinement was performed using the FULLPROF package, and a pseudo-Voigt profile function with preferred orientation correction was used [13]. The bulk density was measured by Archimedes method. The microstructures were observed from the fracture surfaces of these ceramics with a field emission scanning electron microscopy (SEM, S-4800, Hitachi Co., Tokyo, Japan). The dielectric properties and impedance data of the ceramics were evaluated with a broadband dielectric spectrometer (Turnkey Concept 50, Novocontrol Technologies GmbH & Co. KG, Hundsangen, Germany) in a broad range of temperature (128–500 K) and frequency (1 Hz to 10 MHz) with a heating rate of 2 K/min, and the silver paste was adopted as electrode.

3. Results and discussion

The sintering behavior of $Nd_2NiO_{4+\delta}$ ceramics during spark plasma sintering process is shown in Fig. 1. A rather large thermal expansion is observed at the temperature ranges from room temperature to about 700 °C. The shrinkage initiates at about 700 °C, and it persists in the front of soaking period at 950 °C, then it disappears when the soaking time goes beyond 2 min, suggesting that the densification process is almost complete. The inset of Fig. 1 shows the sintering time dependence of vacuum in the furnace chamber, there is a sharp peak on the curve. The peak temperature is about 900 °C. The sharp decrease of the vacuum in the chamber indicates some gases emit from the sample. The same sintering behavior has been observed in the $La_{1.75}Ba_{0.25}NiO_4$ ceramics, and this peak should be attributed to the emission of the interstitial oxygen, which has come from the air during the calcining process as pointed by the previous work [14]. Although the oxygen in air may infiltrate into the lattice to form interstitials again during the post-annealing process as found by Takeda et al. [15], the content of excess oxygen in the spark plasma sintered sample is lower than that in conventional solid-state sintered sample. This low content of excess oxygen is responsible for the stable and creditable dielectric data of spark plasma sintered sample.

Much work has shown that the crystal structure is sensitive to the content of interstitial oxygen, and so the oxygen content could be roughly determined by the structure data [5,6]. Fig. 2 shows the XRD pattern of $Nd_2NiO_{4+\delta}$ ceramics at room temperature and the crystal structure is refined by Rietveld method. There are two secondary phases, i.e., Nd_2O_3 and NiO, besides the main $Nd_2NiO_{4+\delta}$ phase, and the abundances of these two secondary phases are 4.82(9) wt% and 1.99(17) wt%, respectively. The reliabilities of refinement are shown as following: R_p(profile) = 6.31%, R_{wp}(weighted profile) = 8.43%, and χ^2(goodness of fitting) = 2.51. The space group of main $Nd_2NiO_{4+\delta}$ phase is *F mmm* (69), and the cell parameters are $a = 5.3748(3)$ Å, $b = 5.4620(3)$ Å, and $c = 12.3719(6)$ Å, respectively. This space group implies high content of excess oxygen in the present ceramics [6,15]. At final step of the Rietveld refinement, the occupancy of apical oxygen is refined as 1.096(20), and this means the content of excess oxygen, δ in $Nd_2NiO_{4+\delta}$ phase, is about 0.192. This result is similar to that of the previous work [6], and so the present result is reliable.

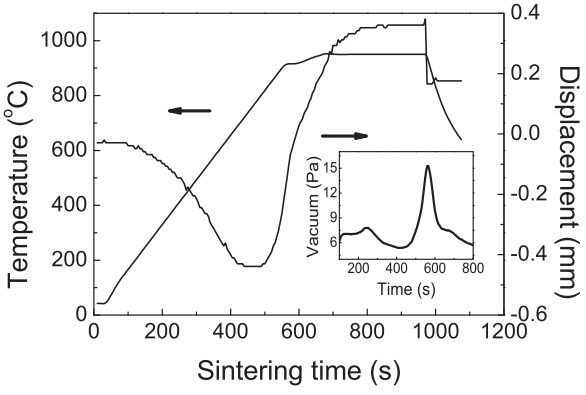

Fig. 1. Shrinkage curve and sample's temperature as a function of sintering time during spark plasma sintering process of $Nd_2NiO_{4+\delta}$ ceramics. The inset is the furnace chamber's vacuum during the SPS process.

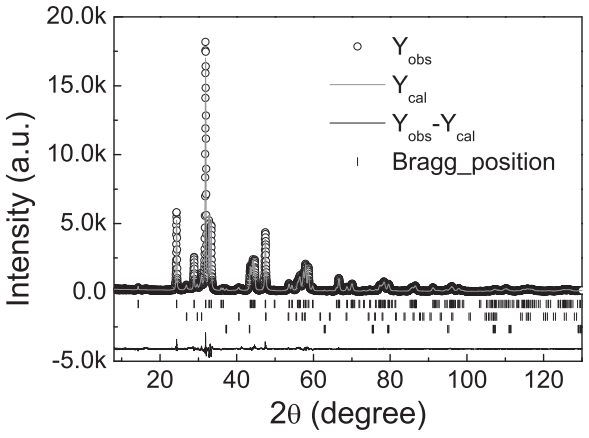

Fig. 2. Rietveld analysis results of XRD patterns for $Nd_2NiO_{4+\delta}$ ceramics at room temperature. Vertical marks show the positions of allowed Bragg reflections for $Nd_2NiO_{4+\delta}$, Nd_2O_3 and NiO from top to bottom, respectively. A difference curve is plotted at the bottom of the patterns.

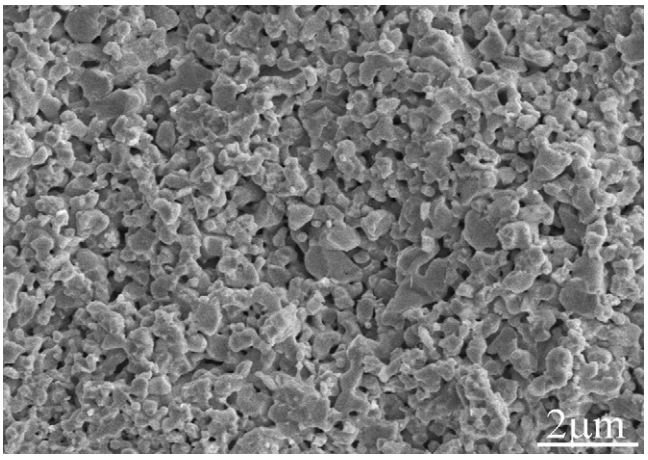

Fig. 3. SEM micrograph of the fracture surface for $Nd_2NiO_{4+\delta}$ ceramics.

Fig. 3 shows the micrograph of the fracture surface for $Nd_2NiO_{4+\delta}$ ceramics at room temperature. The relative dense ceramics are obtained, and the bulk density of the present ceramics is 7.13 g/cm^3, which is about 95% of the theoretic density estimated by the above XRD analysis. The grain size is smaller than 1 μm, and its distribution is not so uniform.

The temperature-dependent of dielectric properties of the present ceramics are shown in Fig. 4. The giant dielectric constant, $\varepsilon' \sim 10^5$, over a wide temperature (200–500 K) and frequency (10 kHz to 5 MHz) range is observed in the present ceramics, and tan δ is moderate at high frequency. Upon cooling the temperature down to 150 K, a sharp decrease of dielectric constant is observed, and the dropping temperature increases with increasing the applied frequency. Also, a peak at the corresponding temperature is appeared on the curve for the temperature dependence of tan δ. This is a typical of dielectric relaxation, and it is the common feature of giant dielectric constant materials [8–12]. According to the previous work [4,7], the charge ordering temperature of $Nd_2NiO_{4.192}$ ceramics is about 150 K, which is coincided with the temperature of dielectric relaxation. This may indicate the correlation between dielectric relaxation and charge ordering in the present ceramics.

To deeply insight the low temperature dielectric relaxation, the frequency dependence of dielectric constants at low temperatures are shown in Fig. 5a. Dielectric constant varies slightly at low frequency, and then it decreases sharply when the frequency is beyond a critical frequency, and the critical frequency increases with increasing the temperature. Then the polydispersion Debye equation [16]

$$\varepsilon^* = \varepsilon' - i\varepsilon'' = \varepsilon_\infty + \frac{\varepsilon_0 - \varepsilon_\infty}{1 + (i\varpi\tau)^{1-\alpha}} \quad (1)$$

is used to fit the $\varepsilon' \sim f$ curves (Fig. 5a). Where, ε_0 is the static dielectric constant, ε_∞ is the dielectric constant at very high frequencies, ω is the angular frequency, τ is the mean relaxation time and α represents the degree of the distribution of relaxation time τ. By fitting these curves, the relaxation times τ at different temperatures are obtained and plot as the function of the reciprocal temperature. The variation of relaxation times with temperature follows the Arrhenius law,

$$\tau = \tau_0 \exp\left(\frac{E_a}{k_B T}\right), \quad (2)$$

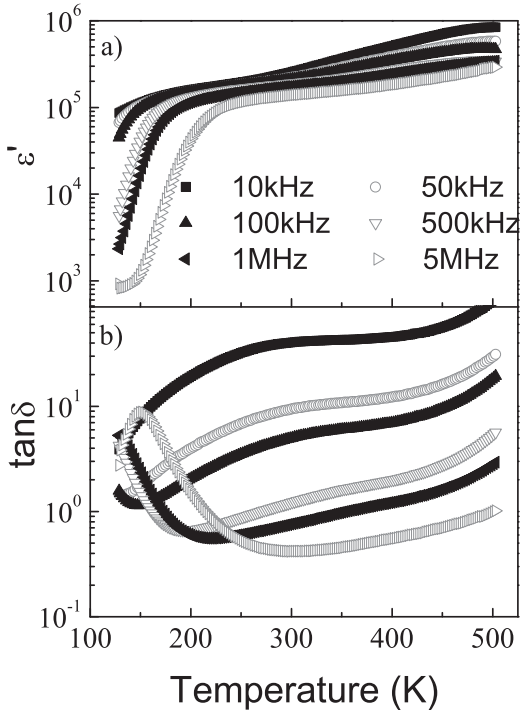

Fig. 4. Temperature dependence of (a) dielectric constant and (b) loss of $Nd_2NiO_{4+\delta}$ ceramics at various frequencies.

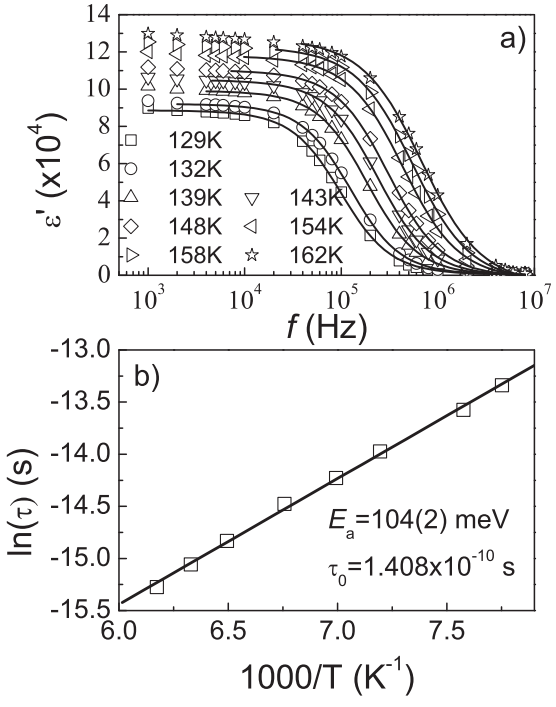

Fig. 5. (a) Frequency dependence of dielectric constant for $Nd_2NiO_{4+\delta}$ ceramics at various temperatures. The solid line is polydispersion Debye fitting. (b) The Arrhenius fitting of relaxation times extracted from the Debye fitting.

where τ_0 is the relaxation time at very high temperatures, E_a is the activation energy, and k_B is the Boltzmann constant. The fitting parameters are obtained as $E_a = 104 \pm 2$ meV and $\tau_0 = 1.41 \times 10^{-10}$ s. The activation energy is almost same as that of $Sm_{1.5}Sr_{0.5}NiO_4$ ceramics [9], and this indicates the same mechanism will be responsible for the dielectric relaxation in these two materials. Combined the low activation energy (~0.1 eV) of dielectric relaxation and the low activation frequency (5 MHz), the dielectric relaxation should be attributed to the polaronic hopping process [17].

To find out the origin of dielectric relaxation in the present ceramics, the effect of electrode should be discussed firstly [18,19]. As shown in the previous work [10,12,20], other factors should be responsible to the giant dielectric response although the interface effect of electrode is indeed existed in the present ceramics. According to the previous work [8,9,20], the dielectric relaxation is closely related to the electrical conduction in nickelates. If one wants to analyse the conductive mechanism, the contributions from bulk and grain boundary should be separated firstly. The analysis of impedance spectra is a good way to do this work. For a typical electroceramics, the equivalent circuit consisting of two parallel *RC* elements connected in series with one *RC* element, $R_{gb}C_{gb}$, representing the grain boundary regions and the other one, R_bC_b, representing the bulks, is usually used to fit the experiment data [21]. Fig. 6a shows the frequency dependences of the imaginary impedance at various temperatures. The above-mentioned equivalent circuit is used to fit the experimental data, and the fitting results are shown as the solid lines in Fig. 6a. From this fitting, the electrical resistivities of bulk and grain boundary for the present ceramics at various temperatures are obtained, and the results are shown as dots in Fig. 6b. As shown in the previous work [3,8,9], the electrical conductive mechanism should be the adiabatic small polaronic hopping process. So, the experimental data are fitting by this mechanism, and the results are shown as solid lines in Fig. 6b. The variation of resistivities of the present ceramics with temperatures indeed obeys the adiabatic small polaronic hopping conductive mechanism in the considered temperature range, and the activation energy of grain boundaries is 77.9 ± 0.6 meV, while that of bulk is 123 ± 1 meV. The activation energy of bulk resistivities is just a bit larger than that of dielectric relaxation, while that of grain boundary is smaller. In the polaronic scenario [22], the activation energy required for electrical conduction due to a hopping process of small polarons is the sum of the hopping energy, which is equal to that of the dielectric relation, and half of the potential difference between a free polaron and a polaron bound to a trap. So the activation energy of electrical conduction should be larger than that of dielectric relaxation. Combined with results of the previous work [8,9,20], we conclude the giant dielectric response should be mainly attributed to the adiabatic small polaronic hopping process in the present ceramics, and small polarons are formed through holes (Ni^{3+}) polarization due to strong electron–phonon interactions in nickelates [8]. Actually, a polaronic hopping model also has been proposed to reconcile the debated views about the origin of the giant dielectric response in $CaCu_3Ti_4O_{12}$ materials [23]. Upon cooling down to the charge ordering temperature (~150 K), the holes will segregate to form the static charge stripes, and they will become inactive with the high frequency external field due to the slow dynamics of static stripes. This results in a degeneration of dielectric response in the present ceramics as shown in Fig. 4.

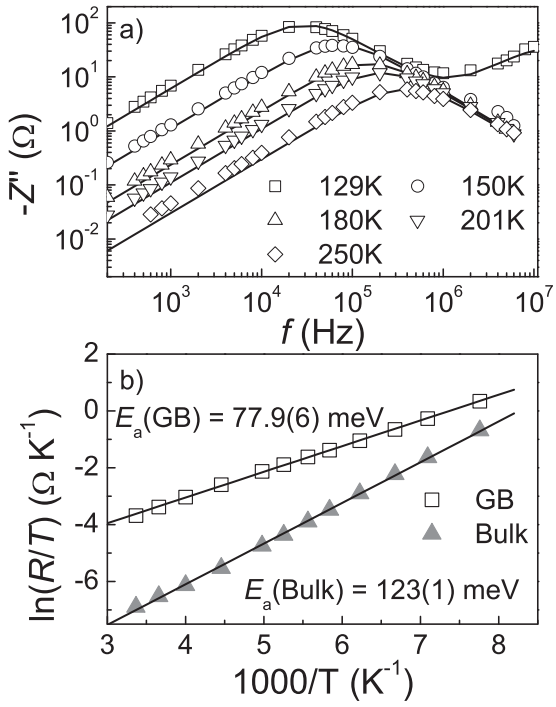

Fig. 6. (a) Variations of imaginary impedance Z'' with frequency at various temperatures, and (b) thermally activated small polaronic hopping fitting of the electrical resistances obtained from the impedance spectra of $Nd_2NiO_{4+\delta}$ ceramics.

4. Conclusion

An oxygen-excess compound $Nd_2NiO_{4.192}$ with minor secondary phases has been prepared by spark plasma sintering. The temperature-stable giant dielectric constant is discovered in the present ceramics up to high frequencies (up to 5 MHz) over a broad temperature range, and the present ceramics are the promising candidates for high frequency applications. One dielectric relaxation around the charge ordering temperature is observed in the present ceramics, and the relaxation should be attributed to the adiabatic small polaronic hopping process, while the polaronic hopping process is closely related to the stripe ordering. From this work, the correlation between the giant dielectric response and charge ordering is confirmed in the oxygen-excess nickelate compound.

Acknowledgments

This work was supported by the National Science Foundation of China under Grant Nos. 50702049 and 50832005, and the Fundamental Research Funds for Central Universities under Grand No. 2010QNA4006.

References

[1] Y. Tokura, Critical features of colossal magnetoresistive manganites, Rep. Prog. Phys. 69 (2006) 797–851.

[2] K.F. Wang, J.M. Liu, Z.F. Ren, Multiferroicity: the coupling between magnetic and polarization orders, Adv. Phys. 58 (2009) 321–448.

[3] G. Wu, J.J. Neumeier, Small polaron transport and pressure dependence of the electrical resistivity of $La_{2-x}Sr_xNiO_4$ ($0 \leq x \leq 1.2$.), Phys. Rev. B 67 (2003) 125116.

[4] K. Ishizaka, Y. Taguchi, R. Kajimoto, H. Yoshizawa, Y. Tokura, Charge ordering and charge dynamics in $Nd_{2-x}Sr_xNiO_4$ ($0.33 \leq x \leq 0.7$), Phys. Rev. B 67 (2003) 184418.

[5] M. Hücker, K. Chung, M. Chand, T. Vogt, J.M. Tranquada, D.J. Buttrey, Oxygen and strontium codoping of La_2NiO_4: room temperature phase diagrams, Phys. Rev. B 70 (2004) 064105.

[6] K. Ishikawa, K. Metoki, H. Miyamoto, Orthorhombic-orthorhombic phase transitions in $Nd_2NiO_{4+\delta}$ ($0.067 \leq \delta \leq 0.224$), J. Solid State Chem. 182 (2009) 2096–2103.

[7] R. Kajimoto, K. Ishizaka, H. Yoshizawa, Y. Tokura, Spontaneous rearrangement of the checkerboard charge order to stripe order in $La_{1.5}Sr_{0.5}NiO_4$, Phys. Rev. B 67 (2003) 014511.

[8] X.Q. Liu, S.Y. Wu, X.M. Chen, H.Y. Zhu, Giant dielectric response in two-dimensional charge-ordered nickelate ceramics, J. Appl. Phys. 104 (2008) 054114.

[9] X.Q. Liu, Y.J. Wu, X.M. Chen, H.Y. Zhu, Temperature-stable giant dielectric response in orthorhombic samarium strontium nickelate ceramics, J. Appl. Phys. 105 (2009) 054104.

[10] S. Krohns, P. Lunkenheimer, Ch. Kant, A.V. Pronin, H.B. Brom, A.A. Nugroho, M. Diantoro, A. Loidl, Colossal dielectric constant up to gigahertz at room temperature, Appl. Phys. Lett. 94 (2009) 122903.

[11] M. Filippi, B. Kundys, S. Agrestini, W. Prellier, H. Oyanagi, N.L. Saini, Charge order, dielectric response, and local structure of $La_{5/3}Sr_{1/3}NiO_4$ System, J. Appl. Phys. 106 (2009) 104116.

[12] P. Lunkenheimer, S. Krohns, S. Riegg, S.G. Ebbinghaus, A. Reller, A. Loidl, Colossal dielectric constants in transition-metal oxides, Eur. Phys. J. Special Top. 180 (2010) 61–89.

[13] J. Rodriguez-Carvajal, Recent advances in magnetic structure determination by neutron powder diffraction, Physica B 192 (1993) 55–69.

[14] C.L. Song, Y.J. Wu, X.Q. Liu, X.M. Chen, Dielectric properties of $La_{1.75}Ba_{0.25}NiO_4$ ceramics prepared by spark plasma sintering, J. Alloy Compd. 490 (2010) 605–609.

[15] Y. Takeda, M. Nishijjima, N. Imanishi, R. Kanno, O. Yamamoto, M. Takano, Crystal chemistry and transport properties of $Nd_{2-x}A_xNiO_4$ (A = Ca, Sr, or Ba, $0 \leq x \leq 1.4$), J. Solid State Chem. 96 (1992) 72–83.

[16] K.S. Cole, R.H. Cole, Dispersion and absorption in dielectrics I. Alternation current characteristics, J. Chem. Phys. 9 (1941) 341–351.

[17] L. Zhang, Z.J. Tang, Polaron relaxation and variable-range-hopping conductivity in the giant-dielectric-constant material $CaCu_3Ti_4O_{12}$, Phys. Rev. B 70 (2004) 174306.

[18] P. Lunkenheimer, R. Fichtl, S.G. Ebbinghaus, A. Loidl, Nonintrinsic origin of the colossal dielectric constants in $CaCu_3Ti_4O_{12}$, Phys. Rev. B 70 (2004) 172102.

[19] M. Filippi, B. Kundys, R. Ranjith, A.K. Kundu, W. Prellier, Interfacial contribution to the dielectric response in semiconducting $LaBiMn_{4/3}Co_{2/3}O_6$, Appl. Phys. Lett. 92 (2008) 212905.

[20] X.Q. Liu, Y.J. Wu, X.M. Chen, Giant dielectric response and polaronic hopping in charge-ordered $Nd_{1.75}Sr_{0.25}NiO_4$ ceramics, Solid State Commun. 150 (2010) 1794–1797.

[21] D.C. Sinclair, A.R. West, Impedance and modulus spectroscopy of semiconducting $BaTiO_3$ showing positive temperature coefficient of resistance, J. Appl. Phys. 66 (1989) 3850–3856.

[22] E. Iguchi, H. Nakatsugawa, K. Futakuchi, Polaronic conduction in $La_{2-x}Sr_xCoO_4$ ($0.25 \leq x \leq 1.10$) below room temperature, J. Solid State Chem. 139 (1998) 176–184.

[23] P.R. Bueno, R. Tararan, R. Parra, E. Joanni, M.A. Ramírez, W.C. Ribeiro, E. Longo, J.A. Varela, A polaronic stacking fault defect model for $CaCu_3Ti_4O_{12}$ material: an approach for the origin of the huge dielectric constant and smeiconduction coexistent features, J. Phys. D: Appl. Phys. 42 (2009) 055404.